A chemical and microbial characterization of selected mud volcanoes in Trinidad reveals pathogens introduced by surface water and rain water

Dirk Schulze-Makuch https://orcid.org/0000-0002-1923-9746, Shirin Haque https://orcid.org/0000-0002-9158-7091, Denise Beckles, Philippe Schmitt-Kopplin https://orcid.org/0000-0003-0824-2664, Mourad Harir, Beate Schneider, Christine Stumpp https://orcid.org/0000-0001-9041-2735, Dirk Wagner https://orcid.org/0000-0001-5064-497X

DOI
10.1016/j.scitotenv.2019.136087

Original publication date
13 December 2019 (Available online)

Document version
Accepted manuscript

Published in
Science of The Total Environment

Citation
Schulze-Makuch D, Haque S, Beckles D, Schmitt-Kopplin P, Harir M, Schneider B, et al. A chemical and microbial characterization of selected mud volcanoes in Trinidad reveals pathogens introduced by surface water and rain water. Science of The Total Environment. 2020;707:136087.

A Chemical and Microbial Characterization of Selected Mud Volcanoes in Trinidad Reveals Pathogens Introduced by Surface Water and Rain Water

Dirk Schulze-Makuch[1,2,3], Shirin Haque[4], Denise Beckles[4], Philippe Schmitt-Kopplin[5,6], Mourad Harir[5,6], Beate Schneider[2#], Christine Stumpp[7,8], and Dirk Wagner[2,9]

Affiliations

[1]Astrobiology Group, Center for Astronomy and Astrophysics, Technische Universität Berlin, Hardenbergstr. 36, 10623 Berlin, Germany
[2] GFZ German Research Centre for Geosciences, 14473 Potsdam, Germany
[3]Department of Experimental Limnology, Leibniz Institute of Groundwater Ecology and Inland Fisheries (IGB), 16775 Stechlin, Germany
[4] University of The West Indies, St. Augustine, Trinidad and Tobago
[5] Research Unit Analytical Biogeochemistry, Department of Environmental Sciences, Helmholtz Zentrum München, Ingolstädter Landstrasse 1, D-85764 Neuherberg, Germany
[6] Analytical Food Chemistry, Technische Universität München, Maximus-von-Imhof-Forum 2, 85354 Freising, Germany
[7] Institute of Groundwater Ecology, Helmholtz Zentrum München, 85764 Neuherberg, Germany
[8] Institute for Soil Physics and Rural Water Management, University of Natural Resources and Life Sciences Vienna, 1190 Wien, Austria.
[9] University of Potsdam, Institute of Geosciences, 14476 Potsdam, Germany

present affiliation: Federal Institute for Materials Research and Testing (BAM), 12205 Berlin, Germany

Corresponding Author: Dirk Schulze-Makuch, schulze-makuch@tu-berlin.de, tel: +49-30-314-23736

Abstract

Terrestrial mud volcanoes are unique structures driven by tectonic pressure and fluids from the deep subsurface. These structures are mainly found in active tectonic zones, such as the area near the Los Bajos Fault in Trinidad. Here we report a chemical and microbiological characterization of three mud volcanoes, which included analyses of multiple liquid and solid samples from the mud volcanoes. Our study confirms previous suggestions that at least some of the mud volcano fluids are a mixture of deeper salt-rich water and surficial/precipitation water. No apparent water quality differences were found between sampling sites north and south of a major geological fault line. Microbiological analyses revealed diverse communities, both aerobic and anaerobic, including sulfate reducers, methanogens, carbon dioxide fixing and denitrifying bacteria. Several identified species were halophilic and likely derived from the deeper salt-rich subsurface water, while we also cultivated pathogenic species from the Vibrionaceae, Enterobacteriaceae, Shewanellaceae, and Clostridiaceae. These microorganisms were likely introduced into the mud volcano fluids both from surface water or shallow ground-water, and perhaps to a more minor degree by rain water. The identified pathogens are a major health concern that needs to be addressed.

Keywords: isotope, metabolomics, contamination, pathogens, mud volcanoes, fluids

Highlights.

- Mud volcano liquids from Trinidad are a mixture of deep-rooted water and surficial water
- The mixture of water from various reservoirs has a distinct chemical and microbial composition
- All samples collected from the mud volcanoes contain pathogens and mostly human pathogens, inferred to be introduced by surficial water
- Pathogens were also detected in rainwater, but only plant pathogens were confirmed.

1. INTRODUCTION

Mud volcanoes can typically be found along fracture or fault zones that are associated with subduction zones (Dimitrov, 2002; Kopf, 2002; Kioka and Ashi, 2015). Fluids interact with the host rock in the subsurface and then protrude as mud slurries onto Earth´s surface. The environmental impact of mud volcanoes has often been a research focus. The studies tend to investigate three main topics: (i) the impact of the mud and its components on aquatic and terrestrial environments (Plumlee et al., 2008), and (ii) mud volcanoes as a greenhouse gas source, due to methane and carbon dioxide emissions (Sauter et al., 2006), and (iii) microbial organisms associated with the mud slurries (Yakimov et al., 2002; Martinez et al., 2006, Niemann et al. 2006). Mud volcanoes are also used as a window into the deep subsurface biosphere. In some instances, the mud has been shown to have elevated concentrations of trace metals such as arsenic (Liu et al., 2009, 2011, 2013), aluminum, manganese (Bonnano et al., 2012) and mercury (Mieiro et al., 2017). The introduction of the mud itself into waterways increases suspended sediment levels and turbidity and may increase dissolved organic matter resulting in low dissolved oxygen levels, impacting aquatic life (Jennerjahn et al., 2013). Mud volcanoes are also well known for their gas emissions, which includes mostly the greenhouse gas methane, but also carbon dioxide. The contribution of mud volcanoes to the greenhouse gas inventory might be significant, yet it has not traditionally been considered (Chao et al., 2010; Milkov et al., 2003; Kokh et al. 2017).

In addition to these more well-known environmental issues surrounding mud volcano emissions, there is also the consideration of direct human health impact due to the presence of human pathogens in the mud. While it is not likely that the hot ejecta itself would be a source of such organisms (Lösekann et al., 2007), the nutrients in the mud may result in increased microbial growth (Plumlee et al. 2008), and hence a possible increased risk for also finding pathogens. In addition, the mud may mix with rain water, which can be a possible source of pathogens as well. There are a few studies that report pathogen contamination from rainwater

in the Caribbean; most investigated fecal and total coliform taxa in rainwater harvesting systems (Welch et al. 2000; Peters 2011; Saunders et al. 2003). In the Grenadines study (Welch et al 2000) rainwater was found to have no fecal coliform, but did have low counts of total coliform. In all of the Caribbean studies, stored rainwater (barrels, tanks or cisterns) was found to be contaminated with fecal or total coliform, in some instances, at levels high enough to be hazardous. While the detected contamination could also be derived from the contamination of the tanks, other studies found that rainwater can have significant levels of active bacteria (Cho and Jang, 2014; Hu et al. 2017; Kaushik et al. 2014), and could be a mechanism for the transport of pathogens for both humans (Kaushik et al. 2012; Evans et al. 2006) and plants (Constantinidou et al 1990). This study builds upon the previous studies by identifying types of bacterial species present in the mud volcano effluents, both liquid and solid, identifying the sources of the water and potential biogeochemical processes within the different mud volcanoes.

The mud volcanoes selected for this study are located in Trinidad and have been characterized according to their fluid chemistry and variable periods of activity by the seminal papers of Dia et al. (1999) and Deville and Guerlais (2009), respectively. The authors claimed that the mud volcano fluids can be distinguished on the island of Trinidad into two groups based on their chemical and isotopic composition, and that these two groups are geographically divided by a major right lateral wrench fault, the Los Bajos fault line, which also acts as a major drain. Our study had the initial objective to determine whether there was also a difference in microbial composition between locations north and south of the fault line. Thus, we selected two sites located northeast (Digity and Devil´s Woodyard) and one site southwest (Balka Devi) of the Los Bajos fault (Figure 1). Only later we discovered that the mud volcano fluids had significant pathogen loads, which led to a re-focussing of the undertaken study.

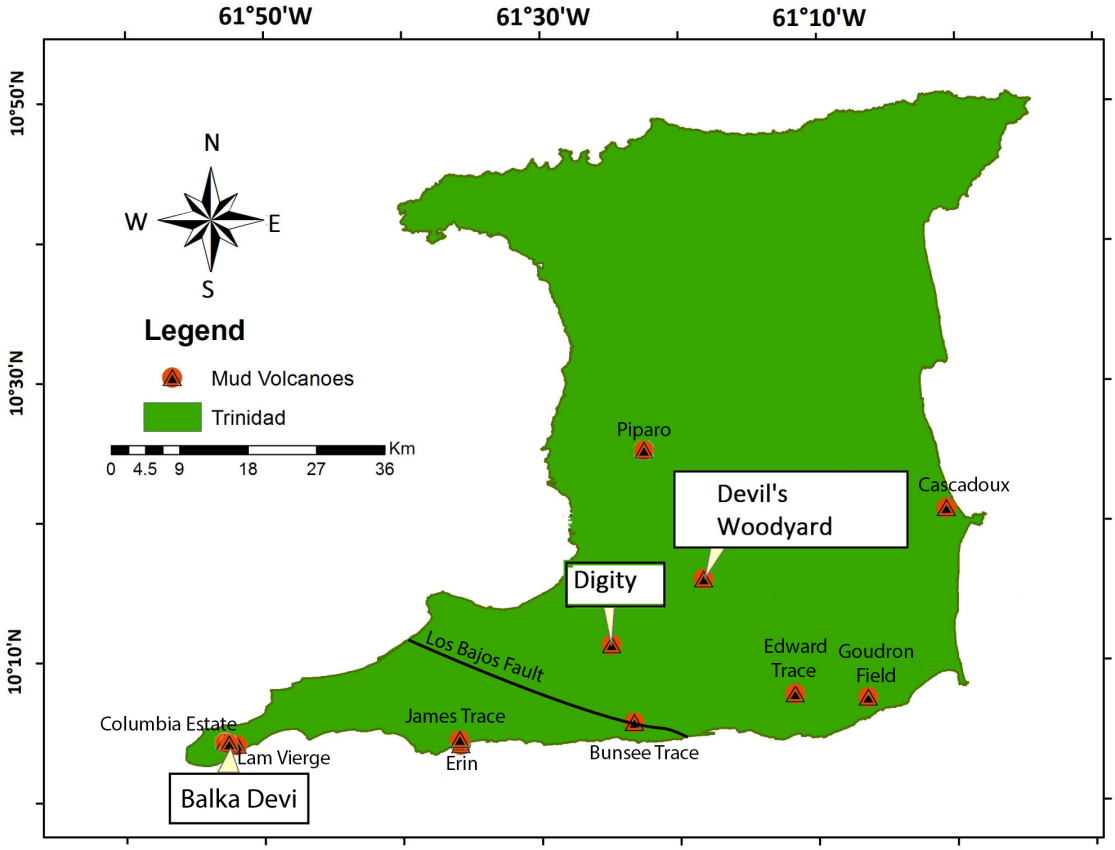

Figure 1. Sampling locations of selected mud volcanoes in Trinidad. Devil´s Woodyard, Digity and Balka Devi were sampled.

2. MATERIALS AND METHODS

2.1 Study Sites

The mud volcanoes in Trinidad belong to a several hundred kilometers-long active belt of active sediment mobilization processes, which occur in the convergent orogen between the Caribbean and the South American plate and are characterized by cyclic phases of activity, ranging from periods of relative quiescence to events of catastrophic magnitude (Deville and Guerlais, 2009; Sundar and Darsan, 2019). Based on elemental, isotopic, and mineralogical analyses, Dia et al. (1999) determined that the fluids from the Trinidad mud volcanoes were originally oceanic, from a reservoir at a depth of more than 3 km within Miocene sediments, but that their chemical composition changed due to high temperature fluid-rock interactions.

143 The selected sample locations were described during the field visit as to their environmental
144 setting and observed fluids (Figures 1 and 2; Table 1). Devils Woodyard was eruptively active
145 and sampled at two locations, one at the surface (DW-1-0), the other at the surface (DW-2-0)
146 and at a depth of 100 cm (DW-2-100). The mud volcano Digity was quiescent during the field
147 season in 2016 and sampled at a depth of 5 cm (Di-5); however, 50 meters from the cone an
148 active location was found in a streambed, which was sampled at the surface (Di-b-0). Finally,
149 three samples were taken from an active site at Balka Devi in close proximity, at the surface
150 (BD-0-L) and at depths from 0-5 cm (BD-0-5-S, BD-0-5-T, see Table 1 for details). All
151 samples were taken using latex gloves and collected in sterilized sampling containers. The
152 temperature of the recovered fluids was measured in the field, while basic chemical
153 parameters such as pH, conductivity, main ions, and stable water isotopes were determined in
154 the laboratory using standard methods. The amount of total petroleum hydrocarbons and oil
155 and grease in the samples was determined in the laboratory.

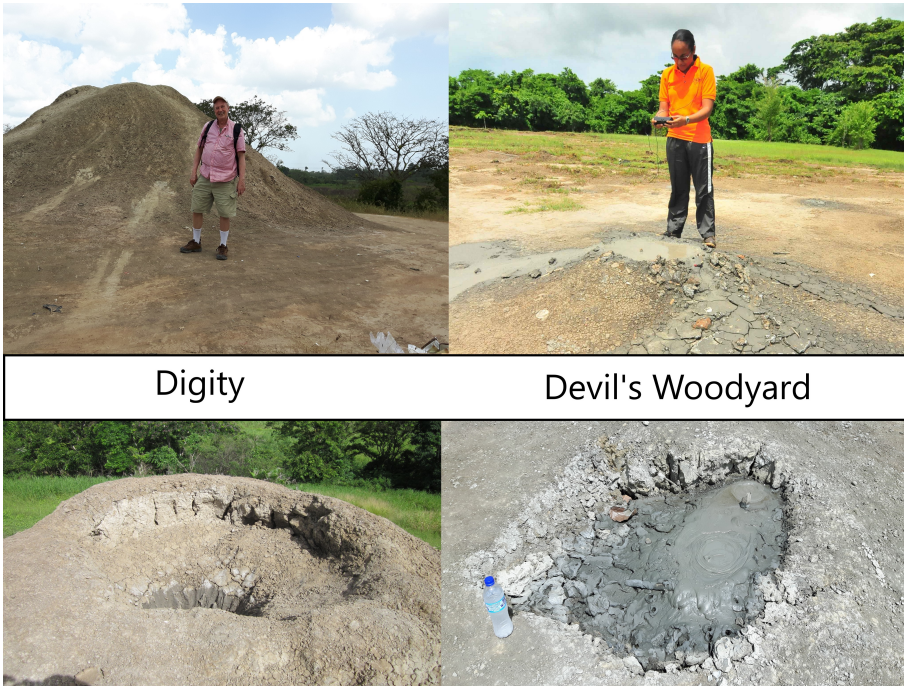

156

157 Figure 2. Photographs of the Digity mud volcano (sample Di-5 was taken 5 cm below the
158 cone of the mud volcano shown in the left image) and one of the mud volcanoes in the Devil´s
159 Woodyard mud volcano field (DW 1).
160

Table 1. Field observations of the collected samples. Devil´s Woodyard (DW), Digity (Di), and Balka Devi (BD)

Sample	Observation
DW-1-0	-Soft Solid -Dark brown in color on the outside, grey on the inside, T= 30.5^{o}C
DW-2-0	-Soft Solid -Dark brown in color on the outside, grey on the inside, T=29.5^{o}C
DW-2-100	-Soft Solid -Dark brown in color on the outside, grey on the inside, T=29.5^{o}C
Di-5	-Top of the mound, dug into the cone and sampled at a depth of 5 cm, moist mud, but not active, hard solid mud - Dark brown in color with white growth patches on surface of sample, possibly fungal in origin
Di-b-0	-About 50 m off the cone, active bubbling, very liquid, T= 28.0^{o}C -Medium brown in color -Sandy texture
BD-0-L	- Very liquid, enclosed in dome-shaped mud structure, T=32.5^{o}C -Medium to light brown in color -Sandy texture
BD-0-5-S	-Caked solid -Sandy texture -Medium to light brown color -Sedimentation observed -Cup holding sample was cracked allowing any liquid in sample to be lost
BD-0-5-T	-Soft Solid -Dark brown in color -Sedimentation observed

2.2 Geochemical analysis

As sample preparation, 5 grams of each sample were mixed with 30 ml of deionized water to form a slurry, from which pH, electrical conductivity, anions and cations were measured. pH-values and electrical conductivity were obtained with a pH-meter and a conductivity meter, respectively. Chloride and nitrate were measured with reference electrodes and prepared standards. The cations were measured using a Block Digester and a FAA Spectrometer, by utilizing standard solutions.

Available phosphorus was determined by dissolving 0.40 g of ammonium molybdate and 0.01 g antimony potassium tartrate in 40 ml of distilled water and diluted to 50 ml. Then 3.00 g of ascorbic acid was dissolved in 40 ml of distilled water and diluted to 50 ml. 0.10 ml of

177 acetone and 15.50 ml of conc. H_2SO_4 were added. Approximately 1.0 g of each sample was
178 weighted in a beaker and 50 ml of distilled water was added to each sample and stirred for 30
179 minutes. Then 0.01916 g of KH_2PO_4 was dissolved in 100 ml of distilled water as standard
180 preparation. 1 ml of this solution was diluted with 100 ml with distilled water. 1 ml of 11 N
181 sulphuric acid and 4 ml of ammonium molybdate-antimony potassium tartrate were added to
182 each sample and standard, and mixed. 2 mL of ascorbic acid solution were added and mixed
183 in. After 5 minutes, the absorbance at 650 nm was measured with a spectrophotometer and the
184 phosphorus concentration was determined from the standard curve.
185
186 Chemical Oxidant Demand (COD) were measured by dissolving 1.02 g of potassium
187 hydrogen phthalate, in 50 ml of distilled water. This produced a 0.1 M solution. Serial
188 dilutions were made to produce solutions of 0.05, 0.025 and 0.0125 M from the 0.1 M
189 solution. Then 2 ml of sample or standard were added to the labelled tubes. Digestion was
190 allowed in the COD reactor for 2 hours. Absorbance was read at a wavelength of 620 nm.
191
192 The amount of total petroleum hydrocarbon was determined by dissolving the extract, which
193 was obtained using US-EPA 1664 method in 50 ml of hexane. 5 g of silica gel (60-200) was
194 added and the mixture was filtered through filter paper containing anhydrous sodium
195 sulphate. A rotary evaporator was used to reduce volume, and the remnants were dried in a
196 70^{o}C oven for 2 hours and weighed. The mass of total petroleum hydrocarbons is the
197 difference between the mass of the initial round bottom flask and the mass of the flask
198 containing the extract.
199
200 U.S. EPA method 1664 was also used to determine total oil and grease. In brief, the 250 ml
201 round bottom flask containing boiling chips was dried in the oven at 100^{o}C for 1 hour, and
202 subsequently in the desiccator before weighing. A Soxhlet apparatus and 200 ml of distilled

hexane were used for further processing. The hexane was just allowed to boil and the extraction was run for 6.5 hours. With a rotary evaporator the excess solvent was removed reducing the volume of the extract. The flask containing the reduced extract was placed in a 70°C oven for 2 hours, then allowed to cool in a desiccator. The weight was recorded. The total oil and grease was the difference between the mass of the initial round bottom flask and the mass of the flask containing the extract. All mud volcano samples were analyzed for these basic chemical parameters except sample DW-2-0.

2.3 Water stable isotope analysis

Water stable isotope analysis was conducted in the mud volcano samples. In two out of seven samples (DW-2-100, BD-0-5-S) free water was available and filtered (0.45 µm) before stable water isotope analysis. In the other samples, sediment pore water was extracted via cryogenic extraction for the analysis of stable water isotopes following common procedures (e.g. Königer et al. 2011; Orlowski et al. 2018). 6-15 g moist sediment was used depending on the expected water content (0.18-0.40 g/g gravimetric water content). Water was extracted at 105°C, and the extraction was completed (≥ 99.3% efficiency) after 105-120 min. The isotope ratios of the water ($^{18}O/^{16}O$ and $^{2}H/^{1}H$) were measured in 0.75 – 1.5 ml water samples by cavity ring-down spectroscopy (Picarro L-2130i). A two-point calibration with laboratory reference material calibrated against VSMOW-SLAP (Vienna Standard Mean Ocean Water-Standard Light Antarctic Precipitation) scale was used. Each sample was measured up to nine times. Precision of the instrument (1σ) was better than 0.1‰ and 0.6‰ for $\delta^{18}O$ and $\delta^{2}H$, respectively. Values are reported as the ratio of isotopes (R_{sample}), given in the delta notation as δ-value (‰), which is the relative deviation of the sample from a standard ($R_{standard}$):

$$\delta(‰) = \frac{R_{Sample} - R_{Standard}}{R_{Standard}} \cdot 1000$$

2.4 FT-ICR Mass Spectrometry

Negative electrospray ionization Fourier transform ion cyclotron resonance [ESI(−)] FT-ICR mass spectra were acquired using a 12T Bruker Solarix mass spectrometer (Bruker Daltonics, Bremen, Germany) and an Apollo II electrospray ionization (ESI) source in negative mode. Pore water from mud volcanoes was processed (after acidification with formic acid) through solid-phase cartridges (Bond Elut PPL, 100 mg, 1 ml, Agilent) to desalt them before electrospray infusion, whereas sediments from mud volcanoes were extracted using toluene solvent. Subsequently, an appropriate concentration of the SPE extracts were prepared in methanol while the toluene extracts were prepared in methanol/ammonium hydroxide for [ESI(−)] FT-ICR-MS analysis. Infusion of samples was done with a microliter pump at a flow rate of 120 µl h^{-1} with a nebulizer gas pressure of 138 kPa and a drying gas pressure of 103 kPa. A source heater temperature of 200 °C was maintained to ensure rapid desolvation of the ionized droplets. The spectra were acquired with a time domain of 4 MW in [ESI(−)], and 500 scans were accumulated for each mass spectrum. All spectra were internally calibrated using appropriate reference mass lists. Data processing was done using Compass Data Analysis 4.0 (Bruker, Bremen, Germany) and formula assignment was made by in-house made software (NetCalc) (Tziotis et al. 2011). Molecular formula assignments were generated based on the exact mass differences using NetCalc software (Tziotis et al. 2011). The assigned molecular formulas were based on a restricted list of selected small molecular units with defined mass differences (Tziotis et al. 2011). Here, the compositional networks enabled assignment of elemental formulas out of mass spectra and allowed alignments according to compositional relationships. The final assigned molecular formulas were categorized into groups containing CHO, CHNO, CHOS, and CHNOS molecular compositions, which were used to reconstruct the group-selective mass spectra. Plots of the assigned molecular formulas retrieved from the FTICR-MS data sets were processed using van Krevelen plots (Schmitt-Kopplin et al. 2010, Handle et al. 2017). FT-ICRMS data were normalized by unit-variance scaling in order to

adjust variances between the samples (Lucio, 2009). A hierarchical clustering approach was performed on the normalized data (Hierarchical Clustering Explorer 3.5, Maryland, USA). Calculation of clusters was done using average linkage and Euclidian metric as similarity search. The process allows to group samples in a homogeneous and distinct cluster without prior knowledge of data classification.

2.5 Microbiological Analyses

Media and cultivation

For the cultivation of aerobic and anaerobic bacteria, TSA (trypticase soy agar, 1/10 strength) was amended with the following salts (per liter): 24.5 g NaCl, 1 g $CaCl_2$, 0.74 g KCl, 2.43 g $MgCl_2$, 6.9 g $MgSO_4$. The pH value was adjusted to 7.8 – 8.0 with 1 M NaOH. To prevent the growth of fungi, cycloheximide (100 µg ml^{-1} final concentration) was added after autoclaving. For anaerobic growth the medium additionally contained 0.5 g sodium thioglycolate as a reducing agent and 0.001 g sodium resazurin as redox indicator. For preparation of the anaerobic medium the ingredients were dissolved in the medium with adjusted pH and afterwards the bottles were sealed with black rubber stoppers and a screw cap with a hole. The bottles were flushed with N_2 for at least 30 min, until the redox indicator (resazurin) turned colorless. The medium was autoclaved with a hypodermic needle placed in the rubber stopper as air valve. After autoclaving the needle was removed immediately. The medium was cooled to about 60°C and transferred into the anaerobic glove box, where cycloheximide was added and the plates were poured and dried. Serial dilutions (in 2% NaCl) of the samples were plated and incubated at 28°C. For growth under anaerobic conditions all steps were carried out in the glove box and the plates were transferred to an anaerobic chamber which was flushed with a mixture of N_2 [80%] and CO_2 [20%] for 10 min. Finally, the gas mixture was added at 1.5 atmospheres of overpressure.

Taxonomic characterization of isolates

DNA of purified isolates was extracted by a simple standard protocol (Jacobsen, 1995). A bacterial colony was suspended in 100 µl destilled water in a 0.2 ml reaction tube and was incubated for 10 min at 98°C in a heating block. After boiling the suspension was cooled on ice immediately and then centrifuged for 10 min, 6000 x g, 4°C. The supernatant contained the DNA. A partial sequence of the 16S ribosomal RNA gene was amplified with the primers 27F and 907R. Sequencing was done by GATC (Konstanz, Germany).

Isolation of total DNA from samples

DNA was isolated in triplicates with the PowerSoil DNA kit (MO BIO Laboratories, USA) applying a modified protocol from Direito et al. (2012). In brief, 0.5 g of soil was weighed into the bead-beating tube from which the buffer was removed previously. Instead, to enhance DNA recovery from the soil matrix, cell lysis was done in a FastPrep cell disrupter in the presence of 1 ml of 1M phosphate buffer, pH 8.0 containing 15 % ethanol and 60 µl solution C1 from the kit. To complete the lysis the tube was incubated in a block heater at 80 °C for 40 min before the first centrifugation. All further steps followed the PowerSoil manual. DNA was eluted with prewarmed (55°C) solution C6.

Quantitative PCR analysis (qPCR)

The qPCR was performed in a CFX Connect Real-Time PCR Detection System (Bio-Rad, CA, USA) in duplicates of total DNA extracted from the sediment samples using iTaq Universal SYBR Green Supermix (Bio-Rad). DNA was amplified with the universal primers 331F and 797R (Nadkarni et al, 2002) and the following cycling parameters: initial denaturation at 95°C, 3 min followed by 40 cycles (95°C, 30 s; 58°C, 30 s; 72°C, 30 s; 80°C, 3 s plus plate read). The correlation coefficient for the standard curves was ≥0.99 and the PCR efficiency was on average 90%. The standard was a known concentration (copy numbers) of a 16S rRNA gene PCR fragment of *Bacillus subtilis.* To measure the abundances of functional

genes DNA was amplified with primers targeting *cbb*L (large subunit gene of ribulose-1,5-bisphosphate carboxylase/oxygenase a marker of carbon dioxide fixing bacteria), *dsr*B (dissimilatory sulfite-reductase beta subunit gene a marker of sulfate-reducing bacteria), *mcr*A (alpha subunit gene of methyl coenzyme M reductase a marker of methanogens also a proxy for *Archaea*), and *nir*S (nitrite reductase gene from denitrifying bacteria). The corresponding primers and cycling parameters were: cbbLR1F/ cbbLR1intR (Selesi et al., 2005, 2007), initial denaturation at 95°C, 3 min followed by 40 cycles (95°C, 15 s; 60°C, 1 min; 80°C, 3 s plus plate read), the standard was a known concentration of the *cbb*L gene fragment of *Xanthobacter autotrophicus*; dsr2060F/dsr4R (Geets et al., 2006), initial denaturation at 95°C, 3 min followed by 40 cycles (95°C, 5 s; 60°C, 30 s; 72°C 10 s; 80°C, 3 s plus plate read), the standard was a known concentration of the *dsr*B gene fragment of *Desulfovibrio vulgaris*; mlasF/mcrAR (Steinberg & Regan, 2008), initial denaturation at 95°C, 3 min followed by 40 cycles (95°C, 5 s; 60°C, 20 s; 72°C 30 s; 80°C, 3 s plus plate read), the standard was a known concentration of the *mcr*A gene fragment of *Methanosarcina barkeri*; nirSnF/nirSnR (Smith et al., 2007), initial denaturation at 95°C, 3 min followed by 40 cycles (95°C, 15 s; 60°C, 1 min; 80°C, 3 s plus plate read), the standard was a known concentration of the nirS gene fragment of *Pseudomonas* sp.

Phospholipid Fatty Acid (PLFA) Analyses

PLFAs are a main component of the membranes of all microbes and were analyzed using the modified Bligh and Dyer method, as described by Smith et al. (1986). PLFAs decompose quickly upon cell death, thus are thought to represent all viable cells in an environmental sample. Some organisms produce specific or signature types of PLFA biomarkers allowing quantification of important microbial functional groups (e.g. iron reducers, sulfate reducers, or fermenters). The relative proportions of these groups of PLFA biomarkers provide a fingerprint of the microbial community (White et al., 1998; Schulze-Makuch et al., 2003).

Terminally-branched saturated PLFA are generally characteristic for Gram-positive bacteria, but also occur in cell membranes of sulfate-reducing bacteria. Monoenoic PLFA occurs in Gram negative bacteria, particularly in those that are fast growing, utilize many carbon sources, and adapt quickly to a variety of environments. Branched monoenoic PLFA is common in obligate anaerobic bacteria, such as sulfate or iron-reducing bacteria. Mid-chain branched saturated PLFAs are typical for *Actinomycete spp*., certain Gram-positive bacteria and sulfate-reducing bacteria. Normal saturated PLFAs commonly occur in less-diverse microbial populations, but provide very little information about their phylogenetic affiliation. Polyenoic PLFA is characteristic for eukaryotic microorganisms.

3. RESULTS

3.1 Basic chemical and isotopic analyses

The pH was alkaline for all mud volcano fluids analyzed independent of the location (Table 2). Nitrate values were particularly high for Di-b-0, which would be consistent with some anthropogenic contamination.

Table 2: pH, conductivity, and main ions

Sample	pH	Electric Conductivity (mS/m)	Nitrate (mM)	Chloride (mM)	Na^+ (mM)	K^+ (mM)
DW-1-0	9.01	2.88	1.7	23.8	55.5	70.8
DW-2-100	9.05	2.84	0.5	49.4	56.8	43.9
Di-5	9.55	1.94	1.1	23.8	50.9	44.3
Di-b-0	9.00	3.11	30.4	23.1	40.0	14.8
BD-0-L	8.80	3.34	1.6	18.5	40.8	29.3
BD-0-5-S	9.23	5.90	3.2	44.9	57.2	65.1
BD-0-5-T	9.70	2.98	0.9	47.9	57.1	58.0

The analyses of organic compounds indicated that all the fluids sampled included hydrocarbons (Table 3), which is consistent with earlier findings by Meckenstock et al. (2014) and indicative that the fluids transverse hydrocarbon-rich areas in the deeper

365 subsurface. The amount of available phosphorus was consistent within all samples with a
366 value of about 0.7 mg/l.

367
368 Table 3: Organic Carbon Analyses
369

Sample	Available Phosphorus* (mg/l)	COD (mg) O_2 (mg)	Mass of Total Petroleum Hydrocarbon (g)	Mass of Total Oil and Grease (g)	Observation of Extract from Oil and Grease Sample
DW-1-0	0.7328	N/A	0.0002	0.0011	Clear
DW-2-100	0.7436	N/A	0.0003	0.0037	Slight Yellow
Di-5	0.6740	N/A	0.0004	0.0083	Slight Yellow
Di-b-0	0.7436	0.1083	0.0253	0.0480	Very Yellow
BD-0-L	0.6610	0.4438	0.0004	0.0021	Slight Yellow
BD-0-5-S	0.6610	N/A	0.0002	0.0011	Clear
BD-0-5-T	0.6610	N/A	0.0005	0.0060	Yellow

370

371 The majority of the samples had similar isotopic composition and clustered close together.
372 These isotopic values were in a similar range of values reported for the same mud volcanoes
373 in Trinidad (Dia et al. 1999) (Figure 3). Exceptions were the water extracted from the solid
374 sediment sample taken at Balka Devi (BD-0-5-S) with an exceptionally high $\delta^{18}O$ value, and
375 the water sample at Digity (Di-b-0) (Table 4). The first (BD-0-5-S) was from a sample with
376 cracked cup and therefore, most likely fractionation processes resulted in large isotope ratios;
377 its initial value remains unknown. The latter (Di-b-0) plots close to an evaporation line
378 indicating surface or rain water as main source.

379
380
381 Table 4: $\delta^{18}O$ and $\delta^{2}H$ (± standard deviation) of water samples from mud volcanoes
382

Sample	$\delta^{18}O$ (‰)	$\delta^{2}H$ (‰)
DW-1-0	3.54 (±0.04)	-14.3 (±0.2)
DW-2-0	3.77 (±0.04)	-9.4 (±0.1)
DW-2-100	n.a.	n.a.
Di-5	3.03 (±0.04)	-1.2 (±0.3)
Di-b-0	4.00 (±0.06)	19.8 (±0.1)
BD-0-L	4.37 (±0.02)	-1.3 (±0.3)
BD-0-5-S	10.89 (±0.07)	20.0 (±0.1)

383

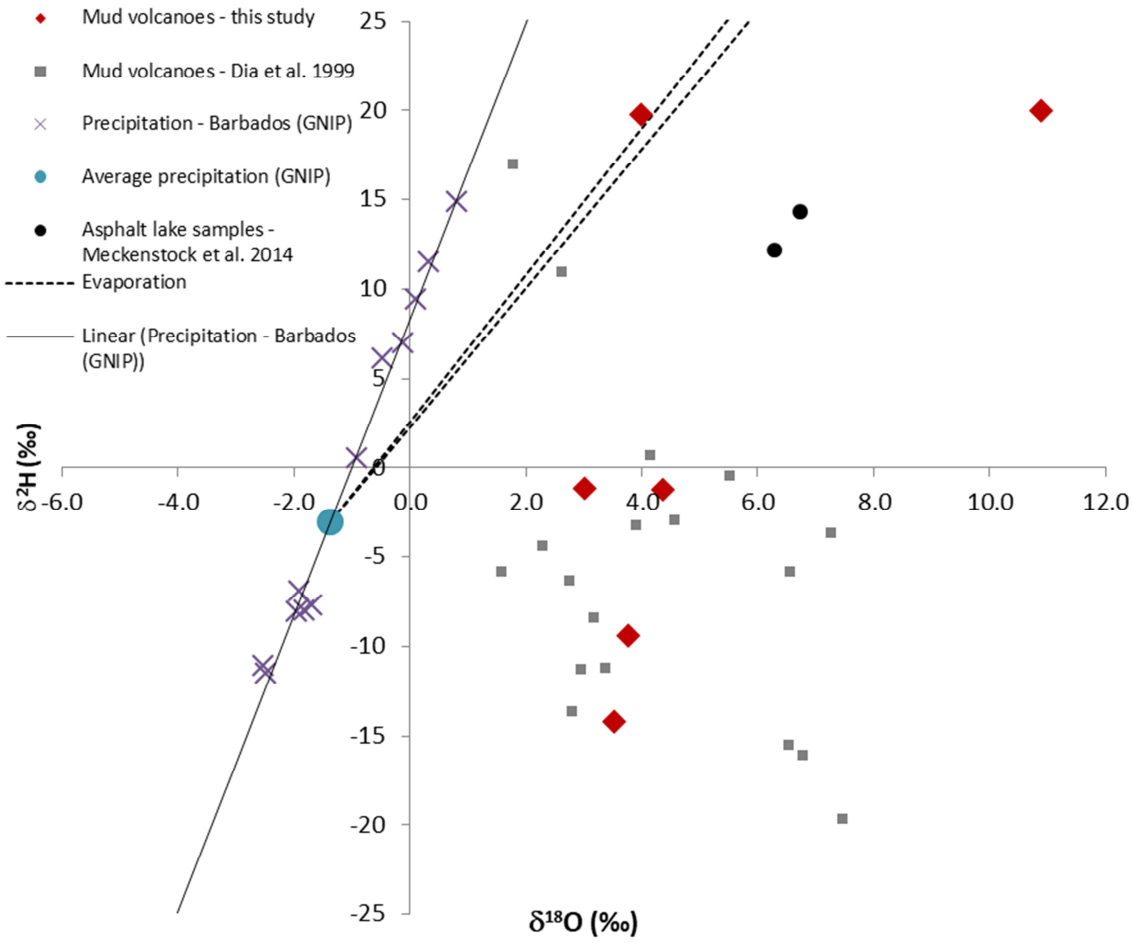

Figure 3: $\delta^{18}O$ and $\delta^{2}H$ of water samples from mud volcanoes (red symbols) in comparison to published data of monthly (purple crosses) and annual averages (blue circle) in precipitation from the closest station of the Global Network of Isotopes in Precipitation (GNIP) database of the International Atomic Energy Agency (IAEA) in Barbados (including the Local Meteoric Water line; black line), other mud volcanoes (grey squares; Dia et al. 1999) and asphalt lake samples (black circles; Meckenstock et al. 2014) from Trinidad. The estimated local evaporation line and its uncertainty range is depicted by the gray dashed lines (Meckenstock et al. 2014).

3.2 Chemical Diversity Characteristics

We examined the water extract of the mud volcano samples, representative of bioavailable and dynamic organic fraction and the toluene extracts more representative of the original organic geochemical signature of the mud-systems. All FTICR-MS spectra were extremely rich in the C, H, N, O, S compositional space and were close to the signature of oxidized asphalts (Figure S1). The van Krevelen diagrams (Figure S1) of toluene extracts showed smooth and widespread distributions over large ranges of unsaturation (H/C ratio), down to

low degrees of oxygenation (small O/C ratio). In contrast, water extracts showed an increase in O/C ratio (i.e. oxidation) with almost unchanged average hydrogen deficit except for Di-b-0 (Figure S1 and Table S1). CHO and CHNO molecular compositions were abundant in both mud volcanoes extracts. However, CHNO and CHOS compounds were specifically significant in Di-b-0, suggesting its unique individual chemical diversity of N,S-functionalized compounds (Table S1, Figure S2). When sorted according to the number of oxygen atoms in assigned CHO, CHNO and CHOS molecular compositions, water extracts showed a near Gaussian distribution as compared to toluene extracts (Figure S2). Thus, sorted oxygen atoms in Balka Devi (BD-0-5-S) and Digity (Di-5) water extracts demonstrated overall congruence of considerable oxygenation, sulfurization and nitrogenation of organic molecules (Figure 2S-B). In addition, hierarchical cluster analysis (HCA) based on the FTICR-MS dataset revealed the specific chemical composition variances across all mud volcano extracts. HCA-based analysis of toluene mud extracts reflects the mineral bond and water insoluble organic compounds and clearly differentiate three main groups: (i) Devil´s Woodyard (DW-1-0, DW-2-0 and DW-2-100), (ii) Balka Devi (BD-0-L, BD-0-5-S) and Digity (Di-5), and (iii) Digity (Di-b-0), respectively (Figure 4A). At this level of classification, chemical diversity in toluene mud extracts varied according to the mud volcano sites in the order of Devil´s Woodyard < Balka Devi ~ Digity (Di-5) < Digity (Di-b-0), and the FTICR MS-based molecular compositions related to this classification are shown in van Krevelen diagrams (Figures 4B-D). All samples from the Devil´s Woodyard site show specifically highly aromatic oxygenated and nitrogen rich CHO and CHNO compounds ($0.5 \leq H/C \leq 1.3$ and $0.1 \leq O/C \leq 0.35$) with weighted average DBE value of 11. While the compositional space in Balka Devi and Digity (Di-5) sites are highly characteristic for only CHO saturated and oxygen rich compounds ($H/C > 1.6$ and $1 \leq H/C \leq 1.6$), Digity (Di-b-0) was covering low oxygen containing compounds over a wide range of saturated and unsaturated molecular ratios ($0.56 \leq H/C \leq 2.33$ and $0.02 \leq O/C \leq 0.33$), which is

characteristic of asphalts (Meckenstock et al. 2014, Handle et al. 2017). In contrast, the water-soluble fraction showed no possible classification to geography. As shown in Figure 5, Digity (i.e., Di-b-0 and Di-5) and Balka Devi (BD-0-5-S) were highly variable in their compositional space, suggesting specific biogeochemical processes. As exception, Balka Devi (BD-0-L) grouped together with Devil´s Woodyard. As shown in Figure 5A, four groups of CHO, CHNO, CHOS and CHNOS compounds with molecular ratios $0.5 \leq H/C \leq 1.5$ and $0.04 \leq O/C \leq 0.5$, $1.5 \leq H/C \leq 2.5$ were observed, suggesting mainly O,N,S-fused aromatic compounds as well as appearance of mostly aliphatic acid compounds and derivatives, respectively (Fig 5B). Unlike, Di-b-0 was essentially rich in linear aliphatic and aromatic compounds with mostly extensively suite of naphthenic acids and derivatives with branched, cyclic and aromatic compounds (Fig 5C) reflecting a biodegradation of the original asphalts. In addition, Balka Devi (BD-0-5-S) and Digity (Di-5) showed specific and individual chemical diversity of O,N,S-functionalized CHO, CHNO and CHOS compounds (Fig 5D and 5E) more specific of oxygen rich terrestrial organic matter.

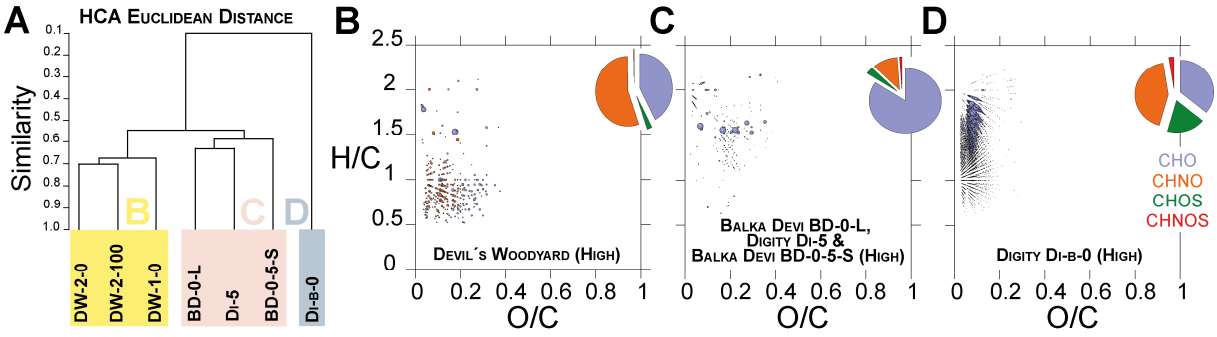

Figure 4. Negative electrospray 12T-FTICR mass data of toluene mud volcanoes sediments extracts. A Clustering diagram based on the similarity values between the spectra of the seven samples using Euclidean distance. B (Devil´s Woodyard), C (Balka Devi, BD-0-L & BD-0-5-S, and Digity "Di-5"), and D (Digity "Di-b-0") show the van Krevelen diagrams of the most abundant mass peaks in each case respectively. Insert histograms represent the molecular series based on CHO (Blue), CHOS (green), CHNO (orange), and CHNOS (red) atom combinations. Bubble size is equivalent to mass peak intensity.

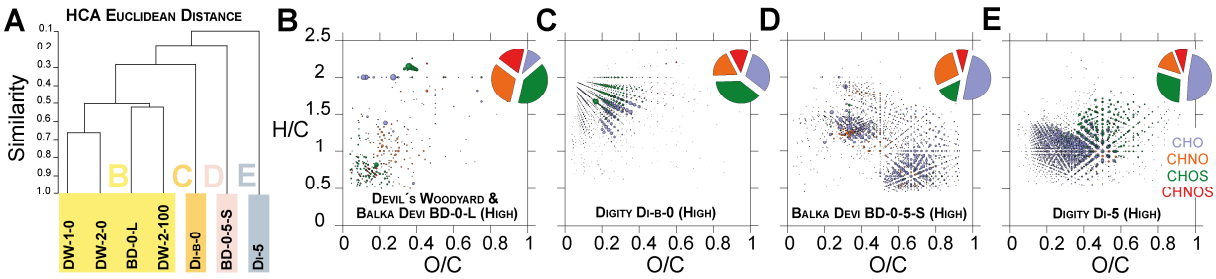

Figure 5. Negative electrospray 12 T FTICR mass data of water-soluble fractions of the mud volcano samples. A Clustering diagram based on the similarity values between the spectra of the seven samples using Euclidean distance. B (Devil´s Woodyard and Balka Devi BD-0-L), C (Digity Di-b-0), D (Balka Devi BD-0-5-S) and E (Digity Di-5) show the van Krevelen diagrams of the most abundant mass peaks in each case respectively. Insert histograms represent the molecular series based on CHO (Blue), CHOS (green), CHNO (orange), and CHNOS (red) atom combinations. Bubble size is equivalent to mass peak intensity.

3.3 Microbiological Characterization

The microbiological analysis consisted of phospholipid fatty acid (PLFA) analyses, culturing, and DNA sequencing. Biomass was also determined via PLFA analyses and revealed that the biomass was the lowest at Devil´s Woodyard with biomass amounts at or below the detection limit of 10^5 cells g^{-1}, while biomass was by about a factor of 100 higher at the other mud volcano sites. Also, there was a much less diverse population at Devil's Woodyard than at Digity and Balka Devi (Table 5). Low biomass and low diversity would generally be consistent with a higher contribution from deep-seated ground water, while a high biomass and diversity would be consistent with surface water or at least mixing with surface water. The sample PAX is collected rain water and provided information on the biomass and microbial diversity of Trinidadian precipitation. The sample Di-5 was sampled 5 cm below the cavity mound of the Digity mud volcano (Fig. 2b), which did not seem to be active at the time of sampling.

Table 5. Phospholipid fatty acid (PLFA) analyses

Sample	Biomass (cells g^{-1} or mL^{-1})	TerBrSats (% abund.)	Monos (% abund.)	BrMonos (% abund.)	MidBrSats (% abund.)	NSats (% abund.)	Polyenoics (% abund.)
DW-1-0	<2.94 x 10^5	0	0	0	0	0	0

DW-2-0	1.12 x 10^5	0	0	0	0	72.94	27.06
DW-2-100	8.82 x 10^5	14.50	26.62	0	0	38.89	19.99
Di-5	1.2 x 10^7	18.88	43.80	1.54	9.50	24.73	1.56
Di-b-0	5.3 x10^7	13.5	48.84	4.54	3.73	23.71	5.68
BD-0-L	1.1 x 10^7	3.73	62.16	0	0.43	33.07	0.59
BD-0-5-S	7.3 x 10^7	16.23	50.36	1.40	2.02	27.33	2.64
PAX[1]	1.6 x 10^6	0	63.45	0	0	31.87	4.68

Note: [1]rain water sample (control)
Legend: TerBrSats (terminal branched saturated) PLFA characteristic for Firmicutes. Monos (monoic) PLFA characteristic for Proteobacteria, BrMonos (branched monoic) PLFA characteristic for aneorobic metal reducers, MidBrSats (mid-branched saturated) PLFA characteristic for sulfate-reducing bacteria and Actinomycetes, NSats (normal saturated) PLFA characteristics for relative "primitive" bacterial biota, and polyenoic PLFA characteristic for eukaryotes. abund. = abundance.

PLFA analyses determine all viable cells, while biomass determinations via culturable cells only consider the fraction of the total bacteria in a sample that can be cultured in a laboratory environment and therefore is lower compared to PLFA analysis. This was also the case with the mud volcano samples for which generally 1 % could be cultured. However, one advantage of culturing the bacteria was that it can be distinguished between aerobic and anaerobic microorganisms. The amount of culturable bacteria, both under aerobic and anaerobic conditions, is shown in Table 6 and Figure 6. The rain water sample (PAX) did not contain any anaerobic bacteria, because these types of bacteria cannot survive long in an oxygenated atmosphere.

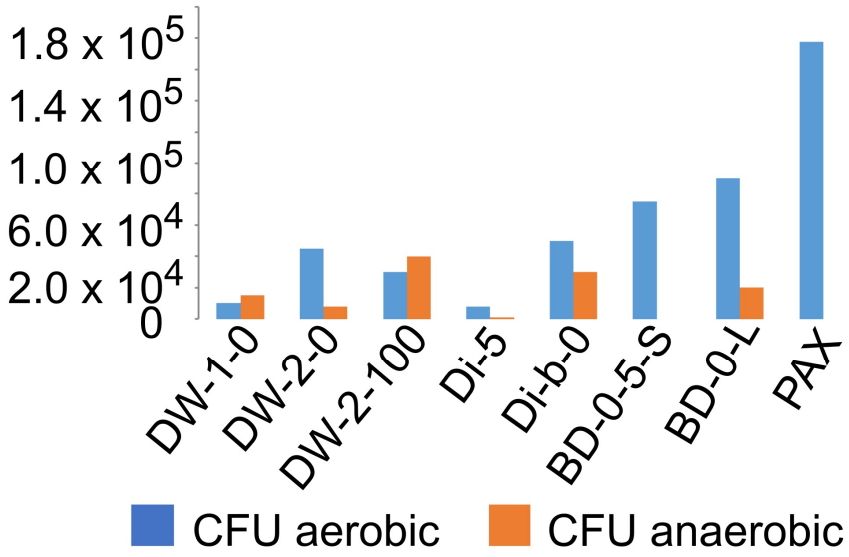

Figure 6. Aerobic vs anaerobic colony forming units (CFUs) per gram or ml of sample at sampling locations Devil's Woodyard DW, Digity Di, and Balka Devi BD.

qPCR analyses using the total DNA recovered, allowed us to detect and quantify functional genes which might be relevant to ecosystems that are anaerobic and influenced by the emission of gaseous compounds like methane and carbon dioxide (Dia et al., 1999). As typical anaerobic microorganisms in those environments we searched for sulfate reducing bacteria, methanogenic archaea, and denitrifiers (Figure 7), and found that sulfate reducing bacteria and methanogenic archaea were present at all sampling locations and depths. A high potential of denitrifying bacteria was only detectable at DW-2 at a depth of 100 cm though nitrate concentration was the lowest (Table 2). The high potential for CO_2-fixing microbes in the samples DW-2-100 and Di-5 might reflect higher CO_2 concentrations.

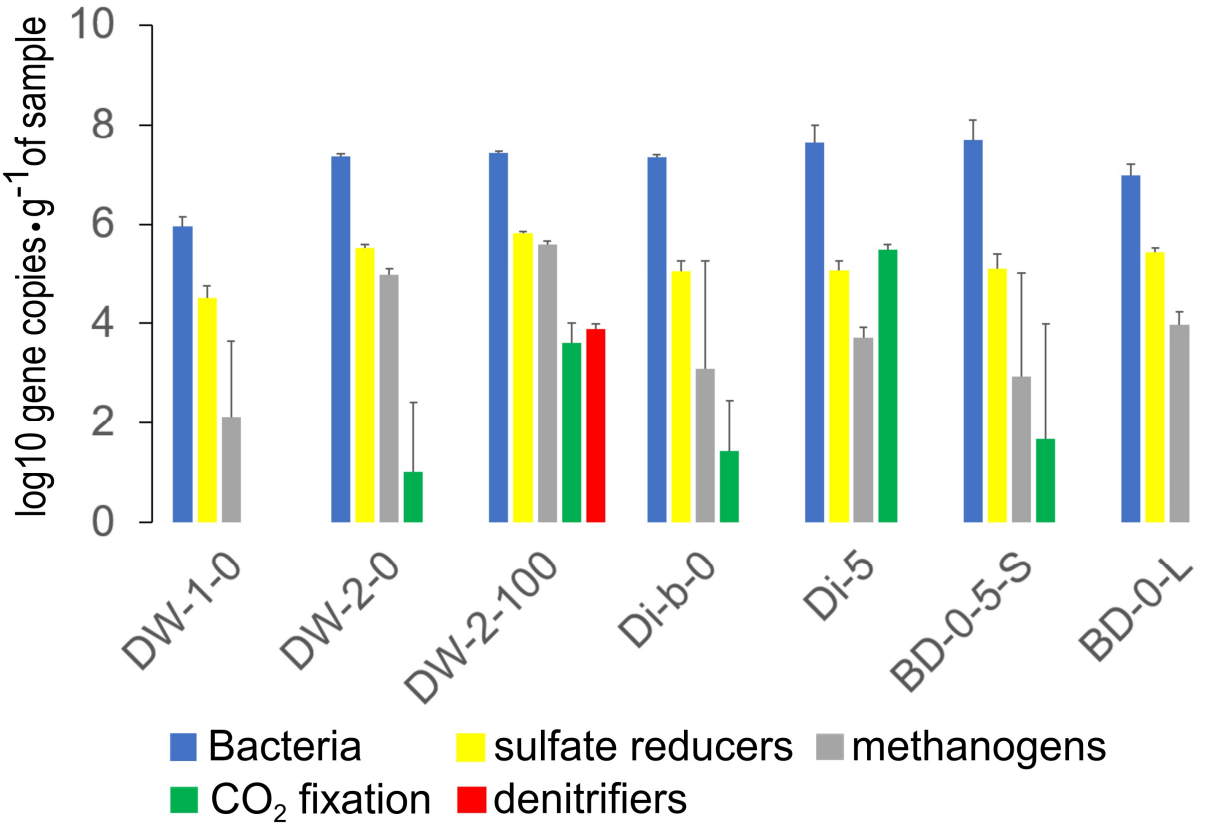

Figure 7. Microbial metabolic diversity within samples based on qPCR. Quantification based on 16S rRNA gene (universal bacteria), *dsrB* gene (sulfate-reducers), *cbbL* gene (CO_2 fixation), *nirS* gene (denitrification), and *mcrA* gene (methanogens)

The 16S rRNA gene analysis revealed further insights into the culturable microbial communities. We discovered several halophilic microorganisms but also many pathogenic strains. The likely pathogenic strains include members of the *Enterobacteriaceae*, *Shewanellaceae*, *Clostridiaceae*, and *Vibrionaceae* (Table 6). Interestingly, there appear to be also pathogenic microorganisms present in the rain water sample (PAX). Control samples collected near the DW and BD mud volcanoes revealed a very different microbial community not consisting of any of the pathogenic species detected in these mud volcano samples (e.g., including instead several *Bacillus* strains such as *B. megaterium*, *B. aryabhattai*, and *B. cereus*).

536 Table 6. Species identification based on cultivation and followed up sequencing of cultured
537 cells. Cultivation was done on TSA (10%) agar + 3.5% sea salts.
538

Isolate		% similarity *	closest gene bank match
Devil's Woodyard (DW)			
Aerobic cultivation			
DW-1-0	MV-5	99	*Vibrio fluvialis*
	MV-6	99	*Labrenzia* sp.
	MV-4	99	*Thalassospira* sp.
	MV-2	99	*Pseudomonas* sp.
	MV-1	99	*Halomonas* sp.
DW-2-0	MV-15	99	*Vibrio sp.*
	MV-13	98	*Marinobacter* sp.
	MV-12	99	*Vibrio fluvialis*
DW-2-100	MV-30	99	*Bacillus* sp.
Anaerobic cultivation			
DW-2-0	Ana-23	99	*Clostridium amygdalinum*
	Ana-20	99	*Shewanella haliotis*
	Ana-29	99	*Vibrio alginolyticus*
DW-2-100	Ana-24	99	*Shewanella fodinae*
	Ana-9	99	*Vibrio alginolyticus*
	Ana-5	98	*Clostridium amygdalinum*
	Ana-11	100	*Enterococcus casseliflavus*
Digity (Di)			
Aerobic cultivation			
Di-5	MV-24	99	*Bacillus* sp.
	MV-23	99	*Nocardiopsis* sp.
	MV-20	99	*Halomonas nitritophilus*
Di-b-0	MV-29	99	*Shewanella haliotis*
	MV-26	99	*Vibrio parahaemolyticus*
	MV-25	100	*Vibrio alginolyticus*
Anaerobic cultivation			
Di5	Ana-25	99	*Halomonas* sp.
Di-b-0	Ana-7	99	*Vibrio natriegens*
	Ana-1	99	*Vibrio* sp.
	Ana-6	99	*Shewanella algae*
	Ana-5	100	*Morganella morganii*
	Ana-10	99	*Vibrio furnissii*
	Ana-14	99	*Vibrio fluvialis*
	Ana-13	100	*Vibrio neocaledonicus*
Balka Devi			
Aerobic cultivation			
BD-05-S	MV-53	100	*Halomonas* cf. *campisalis*
	MV-49	99	*Marinobacter alkaliphilus*
BD-0-L	MV-36	100	*Marinobacter alkaliphilus*

MV-32	99	*Vibrio fluvialis*
MV-38	99	*Rheinheimera* sp.
MV-34	98	*Nitrincola* sp.
Anaerobic cultivation		
BD-0-L Ana-3	99	*Vibrio fluvialis*
PAX *rain water*		
Aerobic cultivation		
PAX-1	99	*Pantoea ananatis*
PAX-2	99	*Pantoea dispersa*
PAX-6	99	*Klebsiella variicola*
PAX-12	99	*Microbacterium* sp.
PAX-13	100	*Enterobacter cloacae/E. ludwigii*

4. Discussion

4.1 Where do the fluids come from?

Geochemical indicators and isotopic fractionation rates are in a similar range of values that were reported previously for the same mud volcanoes in Trinidad (Dia et al. 1999) (Figure 3) and also for other mud volcanoes worldwide as summarized by Mazzini & Etiope (2017). Our results confirm the findings by Dia et al. (1999) that the source area of the mud volcanoes in Trinidad are deep seated seawater reservoirs, but also that a mixing occurs with water from surface near aquifers (Dia et al. 1999). The samples from Devil's Woodyard indicate highest contributions of deep water sources because these sample have the lowest δ^2H (Figure 3) plotting furthest from the local meteoric water line. The deep water source is also in agreement with low biomass in these samples (Table 5). The water extracted from the solid sample from Balka Devi (BD-0-S) is much higher in δ^2H than expected; even higher compared to samples from water droplets enclosed in the nearby pitch lake (Meckenstock et al. 2014). These enriched values cannot be explained by uncertainties of the extraction method (Orlowski et al. 2018), but could be the result of evaporative water loss during storage (broken sampling cup). The sample from the inactive mud volcano (Di-b-0) has different isotopic composition indicative of water with meteoric (rainwater) origin and evaporative loss. Thus, water from surface water origin is the main source which most likely comes from

562 a nearby river occasionally flooding this location. The different water source is supported by
563 the high biomass, the high nitrate and carbon content as well as the different chemical
564 diversity in Di-b-0 compared to other locations.
565
566 No grouping of chemical parameters is evident that would let us to conclude that the Los
567 Bajos Fault has a major role in water quality. This is in line with the analysis of the chemical
568 diversity characteristics that mainly impacted from the original asphalt organics (toluene
569 extract) and terrestrial runoff (water extract). Different types of clustering were apparent
570 according to the extraction protocols. Toluene mud sediment extracts showed that the
571 following three groups (1) DW 1-0, DW 2-0, DW 2-100, (2) Di-5, BD-0-5-S, BD-0-L, and
572 (3) Di-b-0 could be distinguished (Figure 4), while four groups could be distinguished in
573 water extracts (after SPE): (1) DW-1-0, DW 2-0, DW 2-100, BD-0-L, (2) Di-b-0, (3) BD-0-5-
574 S, and (4) Di-5 (Figure 5). The clustering of water extracts (after SPE) corresponds to the
575 grouping from isotope analysis.
576
577 The results from the microbial analyses were distinctly different compared to other mud
578 volcanoes outside of Trinidad (see below), but they conformed in principal to the grouping of
579 water based on chemical and isotopic indicators. There was a stark contrast between the
580 shallow locations at Devil´s Woodyard (DW 1-0 and DW 2-0), where little biomass and
581 microbial diversity was encountered compared to the other sampling sites with a higher
582 biomass and diversity. This points to a deep water source, a hypothesis also supported by the
583 isotope analyses, which indicate a much higher contribution from water sources in the deep
584 subsurface compared to the other sites. However, even here a surface water component cannot
585 be excluded, because we do not know the isotopic composition of the end member (deep
586 water). Based on the PLFA data, the other samples have a much higher biomass and also a
587 rich diversity, which is typical for surface water environments. A revealing sampling location

588 is Di-5, which is within the mound of the currently inactive Digity mud volcano. The sampled
589 microbial community resembles the community from the precipitation water sample mixed
590 within communities from the mud matrix, which is confirmed by the isotope analysis showing
591 that Di-5 has a larger contribution from rain water mixed with groundwater compared to the
592 samples from DW 1-0 and DW 2-0. First, it seems to be surprising that such a diverse and
593 rich community would be the result, but the precipitation data show that even in the rain water
594 there is a startling diverse and rich microbial community (although not as diverse as in Di-5).
595

596 **4.2 An unexpected microbial load**
597
598 Despite specific differences between the individual sampling locations, all our analyzed mud
599 volcano samples contained sulfate reducing bacteria and methanogenic archaea (Fig. 7). They
600 are likely representative of the original fluids from the deep subsurface source before
601 exposure to shallow groundwater. These types of microbes were also found at the Haakon
602 Mosby Mud Volcano at the Barents Sea (Niemann et al., 2006, Lösekann et al., 2007).
603 Sulfate-reducing bacteria were also detected at a mud volcano site in southern Taiwan (Liu et
604 al., 2011), and methanotrophic archaea and various Proteobacteria and Actinobacteria at other
605 mud volcano sites at various locations in the world (e.g. Yakimov et al., 2002, Martinez et al.,
606 2006). In all these sites no microbes were detected that could be identified as pathogens,
607 while all our mud volcano sampling locations were clearly impacted by microbes from
608 shallower (and likely contaminated) water sources. The amount of cultivated bacteria was
609 relatively consistent, both aerobic and anaerobic, when comparing the sampling locations
610 (Figure 6). There were not much differences between the identified microbes in the different
611 sampling locations, which was the case for both non-pathogenic and pathogenic bacteria.
612 Exceptions were carbon dioxide fixating bacteria detected in all mud volcano samples but
613 BD-0-L, and denitrifying bacteria, which were only recovered at DW-2-100. Pathogens were

collected from all environmental samples, even from these sampling locations that did seem to get their water, at least primarily, from a deeper source (DW 1-0 and DW 2-0).

Microbial species identification based on cultivation and followed-up sequencing resulted in many pathogenic strains (Table 6). While even a similarity of nearly 100 % does not necessarily mean that the new isolate is also pathogenic, the evidence from all the identified strains together strongly suggests that the mud volcano samples are substantially impacted by pathogens. *Vibrio* species were detected in all water samples except from the collected rain water samples. While some of the identified *Vibrio* species might be benign, like *Vibrio natriegens*, which is common in estuarine mud, and *Vibrio neocaledonicus,* known for inhibiting corrosion (Moradi et al. 2014), most of them are not. *Vibrio fluvialis*, detected in DW 1-0, DW 2-0, Di-b-0, and BD-0-L, is a pathogen commonly found in coastal environments and is considered an emerging pathogen due to the diarrheal outbreaks it causes (Lee et al. 1981, Ramamurthy et al., 2014). *Vibrio alginolyticus*, detected at DW 2-0, DW 2-100, Di-b-0, is known to cause otitis and wound infections (Longo et al. 2012, Reilli et al. 2011). Also, the *Vibrio* species of *furnissi* and *parahaemolyticus* were found in Di-b-0, both of which cause gastrointestinal illness (EHA 2019, Brenner et al 1983, Daniels et al. 2000, Derber et al. 2011, Ballal et al. 2017).

Other pathogens from water samples were detected as well including *Shewanella haliotis* in DW 2-0 and Di-b-0. This species was first isolated from the gut microflora of edible sea snails (Kim et al. 2007), but more recently has been shown to be the cause of severe skin infections (Poovorawan et al. 2013). *Clostridium amygdalinum,* an environmental, moderately thermophilic anaerobic bacterium which can cause chronic ostitis (Carlier et al. 2006, Parshina et al. 2003) was found in both water samples from DW 2 (at the surface and 100 cm depth). Further, the known pathogen *Enterococcus casseliflavus* was detected at DW-2-100

and *Morganella morganii* at Di-b-0, which is found in intestinal tracts of humans, mammals, and reptiles, but also known to cause urinary infections (Reid et al., 2001; Miller, 2018).

It is instructional to compare the microorganisms collected from rain water with those collected from the mud volcano samples. Neither *Vibrio* species nor any of the before mentioned pathogens were detected in the rain water. However, there were some other bacterial species of concern. These included two *Pantoea* species which belong to the family of the *Enterobacteriaceaea*. One, *Pantoea ananatis* is a known plant pathogen (Coutinho and Venter 2009). Another member of this family, *Enterobacter cloacae*, was also detected. This microorganism has emerged as one of the most commonly found nosocomial pathogens in neonatal units in recent years, with several outbreaks of infection being reported (Dalben et al. 2008). We also cultivated *Klebsiella variicola*, which occurs together with a number of different plants including banana trees and sugarcane, but has also been isolated from cows suffering from bovine mastitis (Podder et al. 2014) and from bloodstream infections (Maatallah et al. 2009).

Whether the pathogens were mixed in directly by water flowing off the surface in the course of extensive rainfall or from surface water/groundwater remains unknown, but given their common occurrence a contamination with surface or near-surface water seems likely. A deeper source of pathogens is unlikely, because (i) the pathogens would have no host in the deep subsurface and (ii) previous isotopic gas analyses resulted in $\delta^{13}C$ methane concentrations ranging between -52 and -33‰, thus implying that the gases are of purely thermogenic nature - although not necessarily the pore water (with the possible exception of Devil´s Woodyard, which might have a slight bacterial component (Deville et al. 2003). Also, (iii) no pathogens were detected at any other mud volcano sites. Instead methanotrophic archaea und sulfate-reducing bacteria seem to be the typical microorganisms present

(Niemann et al., 2006; Yakimov et al., 2002; Martinez et al., 2006; Lösekann et al., 2007; Liu et al., 2011). Further strengthening this conclusion is that some pathogenic strains, albeit plant pathogens (e.g., *Pantoea* sp.) were also identified in collected precipitation water (PAX). Thus rain fall seems to be a major source of pathogenic load. Nevertheless, it appears that the major load of human pathogens derives from shallow ground water or surficial water mixing with the mud volcano fluids.

5. Conclusions

Different types of clustering of chemical components could be observed in liquid and solid mud volcano samples based on chemical analyses including isotopic compositions, but these were not related to their geological location, being north or south of the Los Bajos fault line. Isotopic and microbial analyses revealed that all of the mud volcanoes were chemically and microbially affected by precipitation or surficial water, even when drawing most of the water from deeper sources. In addition to sulfate-reducing bacteria and methanogenic archaea, we could identify pathogenic strains in all samples, including in the sampled rain water, meaning that even precipitation can be a source of pathogenic strains in Trinidad. However, diversity and abundance of pathogenic strains were much higher at sample locations that were in contact with surficial or near-surface ground water. Anthropogenic contamination is not necessarily implicated by our chemical and microbial results, but it is likely occurring at some of the locations. The observed pathogenic load in the environmental samples is a major health concern and should be investigated further.

Acknowledgements

This research was financially supported by ERC Advanced Grant HOME (No. 339231). We also acknowledge the help by Edward Guinan from Villanova University during the sampling campaign (he is pictured in Fig. 2a) and three anonymous reviewers who helped with their constructive comments to improve this paper. Also, we are thankful to Dr. Antonio

Ramkissoon from the University of the West Indies for the culturing of some of the soil samples.

Note

There are no competing interests.

References

Ballal, M., Shetty, V., Bangera, S.R., Prabhu, M., Umakanth, S., 2017. *Vibrio furnissii*, an emerging pathogen causing acute gastroenteritis: a Case Report. JMM Case Rep. 4(9), e005111, doi: 10.1099/jmmcr.0.005111

Bonanno, G., Giudice, R.L., Pavone, P., 2012. Trace element biomonitoring using mosses in urban areas affected by mud volcanoes around Mt. Etna. The case of the Salinelle, Italy. Environmental Monitoring and Assessment 184, 5181–5188.

Brenner, D.J., Hickman-Brenner, F.W., Lee, J.V., Steigerwalt, A.G., Fanning, G.R., Hollis, D.G., Farmer, J.J., Weaver, R.E., Joseph, S.W., Seidler, R.J., 1983. *Vibrio furnissii* (formerly aerogenic biogroup of *Vibrio fluvialis*), a new species isolated from human feces and the environment. Journal of Clinical Microbiology 18 (4), 816–824.

Carlier, J.-P., Manich, M., Loïez, C., Migaud, H., Courcol, R.J., 2006. First isolation of *Clostridium amygdalinum* from a patient with chronic osteitis. J Clin Microbiol. 44(10), 3842–3844. doi: 10.1128/JCM.01200-06

Chao, H.-C., You, C.-F., Sun, C.-H., 2010. Gases in Taiwan mud volcanoes: chemical composition, methane carbon isotopes, and gas fluxes. Applied Geochemistry 25, 428-436.

Cho, B.C., Jang, G.I., 2014. Active and diverse rainwater bacteria collected at an inland site in spring and summer 2011. Atmospheric Environment 94, 409-416.

Constantinidou, H.A., Hirano, S.S., Baker, L.S., Upper, C.D., 1990. Atmospheric dispersal of ice nucleation-active bacteria: the role of rain. Phytopathology 80, 934-937.

Coutinho, T.A. , Venter, S.N., 2009. *Pantoea ananatis*: an unconventional plant pathogen. Mol Plant Pathol. 10, 325-335. doi: 10.1111/j.1364-3703.2009.00542.x.

Dalben, M., Varkulja, G., Basso, M., Krebs, V.L.J., Gibelli, M.A., van der Heijden, I., Rossi, F., Duboc, G., Levin, A.S., Costa, S.F., 2008. Investigation of an outbreak of *Enterobacter cloacae* in a neonatal unit and review of the literature. J. Hosp. Infect.70, 7–14.

741 Daniels, N.A., Shafaie, A., 2000. A review of pathogenic Vibrio infections for clinicians.
742 Infections in Medicine 17, 665–685.
743
744 Derber, C., Coudron, P., Tarr, C., Gladney, L., Turnsek, M., Shankaran, S., Wong, E., 2011.
745 *Vibrio furnissii*: an unusual cause of bacteremia and skin lesions after ingestion of
746 seafood. Journal of Clinical Microbiology 49, 2348–2349. doi:10.1128/JCM.00092-
747 11.
748
749 Deville, E., Battani, A., Griboulard, R., Guerlais, S., Herbin, J.P., Houzay, J.P., Muller, C.,
750 Prinzhofer, A., 2003. The origin and processes of mud volcanism: new insights from
751 Trinidad. Geological Society London, Special Publications 216, 475-490.
752
753 Deville, E., Guerlais, S.-H., 2009, Cyclic activity of mud volcanoes: evidences from Trinidad
754 (SE Caribbean). Marine and Petroleum Geology 26, 1681-1691.
755
756 Dia, A.N., Castrec-Rouelle, M., Boulègue, J., Comeau, P., 1999. Trinidad mud volcanoes:
757 where do the expelled fluids come from? Geochimica et Cosmochimica Acta 63,
758 1023-1038. doi.org/10.1016/S0016-7037(98)00309-3
759
760 Dimitrov, L.I., 2002. Mud volcanoes- the most important pathway for degassing deeply
761 buried sediments. Earth-Science Reviews 59, 49-76.
762
763 Direito, S.O.L., Marees, A., Röling, W.F.M., 2012. Sensitive life detection strategies for low-
764 biomass environments: optimizing extraction of nucleic acids adsorbing to terrestrial
765 and Mars analogue minerals. FEMS Microbiol. Ecol. 81, 111–123. doi:
766 10.1111/j.1574-6941.2012.01325.x
767
768 EHA consulting, 2019. Website https://www.ehagroup.com/resources/pathogens/vibrio-
769 parahaemolyticus/, accessed 11 June 2019.
770
771 Evans, C.A., Coombes, P.J, Dunstan, R.H., 2006. Wind, rain and bacteria: The effect of
772 weather on the microbial composition of roof-harvested rainwater. Water Research 40,
773 37-44.
774
775 Geets, J., Borrernans, B., Diels, L., Springael, D., Vangronsveld, J., Van Der Lelie, D., et al.,
776 2006. DsrB gene-based DGGE for community and diversity surveys of sulfate-
777 reducing bacteria. J. Microbiol. Methods 66, 194–205. doi:
778 10.1016/j.mimet.2005.11.002
779
780 Handle, F., Harir, M., Füssl, J., Koyun, A.N., Grossegger, D., Hertkorn, N., Eberhardsteiner,
781 L., Hofko, B., Hospodka, M., Blab, R., Schmitt-Kopplin, P., Grothe, H., 2017.
782 Tracking ageing of bitumen and its SARA fractions using high-field FT-ICR mass
783 spectrometry. Energy & Fuels 31, 4771-4779.
784
785 Hu, W., Murata, K., Zhang, D., 2017. Applicability of LIVE/DEAD BacLight stain with
786 glutaraldehyde fixation for the measurement of bacterial abundance and viability in
787 rainwater. Journal of Environmental Sciences 51, 202-213.
788
789 Jacobsen, C.S., 1995. Microscale detection of specific bacterial DNA in soil with a magnetic
790 capture hybridization and PCR amplification assay. Applied and Environmental
791 Microbiology 61, 3347-3352.

792
793 Jennerjahn, T.C., Jänen, I., Propp, C., Adi, S., Nugroho, S.P., 2013. Environmental impact of
794 mud volcano inputs on the anthropogenically altered Porong River and Madura Strait
795 coastal waters, Java, Indonesia. Estuarine, Coastal and Shelf Science 130, 152-160.
796
797 Kaushik, R., Balasubramanian R., Dunstan, H., 2014. Microbial quality and phylogenetic
798 diversity of fresh rainwater and tropical freshwater reservoir. PLoS ONE 9, e100737.
799
800 Kim, D., Baik, K.S., Kim, M.S., Jung, B.-M., Shin, T.-S., Chung, G.-H., Rhee, M.S., Seong,
801 N.C., 2007. *Shewanella haliotis sp. nov*., isolated from the gut microflora of abalone,
802 Haliotis discus hannai". Int J Syst Evol Microbiol. 57, 2926–2931.
803 doi:10.1099/ijs.0.65257-0.
804
805 Kioka, A., Ashi, J., 2015. Episodic massive mud eruptions from submarine mud volcanoes
806 examined through topographical signatures. Geophysical Research Letters 42, 8406-
807 8414.
808
809 Koeniger, P., Marshall, J.D., Link, T., Mulch, A., 2011. An inexpensive, fast, and reliable
810 method for vacuum extraction of soil and plant water for stable isotope analyses by
811 mass spectrometry. Rapid Communications in Mass Spectrometry 25, 3041-3048.
812 doi:10.1002/rcm.5198.
813
814 Kokh, S.N., Sokol, E.V., Dekterev, A.A., Kokh, K.A., Rashidov, T.M., Tomilenko, A.A.,
815 Bul'bak, T.A., Khasaeva, A., Guseinov, A., 2017. The 2011 strong fire eruption of
816 Shikhzarli mud volcano, Azerbaijan: a case study with implications for methane flux
817 estimation. Environmental Earth Science, 76: 701.
818
819 Kopf, A., 2002. Significance of mud Volcanism. Review of Geophysics 40, 2-1 – 2-52.
820
821 Lee, J.V., Shread, P., Furniss, A.L., Bryant, T.N., 1981. Taxonomy and description of *Vibrio*
822 *fluvialis sp. nov*. (synonym group F. vibrios, group EF6). Journal of Applied
823 Microbiology 50, 73–94. doi:10.1111/j.1365-2672.1981.tb00873.x
824
825 Liu, C.-C., Jean, J.-S., Nath, B., Lee, M.-K., Hor, L.-I., Lin, K.-H., Maitya, J.P., 2009.
826 Geochemical characteristics of the fluids and muds from two southern Taiwan mud
827 volcanoes: Implications for water–sediment interaction and groundwater arsenic
828 enrichment. Applied Geochemistry 24,1793-1802.
829
830 Liu, C.-C., Maitya, J.P., Jean, J.-S., Sracek, O., Kar, S., Li, Z., 2011. Biogeochemical
831 interactions among the arsenic, iron, humic substances, and microbes in mud
832 volcano.es in southern Taiwan. Journal of Environmental Science and Heath 46, 1218-
833 1230.
834
835 Liu, C.-C., Maitya, J.P., Jean, J.-S., Li, Z., Kar, S., Sracek, O., Yang, H.-J., Chen, C.Y., Selim
836 Reza, A.H.M., Bundschuh, J., Lee, C.-Y., 2013. The geochemical characteristics of the
837 mud liquids in the Wushanting and Hsiaokunshui mud volcano region in southern
838 Taiwan: implications of humic substances for binding and mobilization of arsenic.
839 Journal of Geochemical Exploration 128, 62-71.
840
841 Longo, D., Fauci, A.S., Kasper, D.L., 2012. Harrison's Principles of Internal Medicine, 18th
842 edition, McGraw-Hill Professional.

Lösekann, T., Knittel, K., Nadalig, T., Fuchs, B., Niemann, H., Boetius, A., Amann, R., 2007. Diversity and abundance of aerobic and anaerobic methane oxidizers at the Haakon Mosby mud volcano, Barents Sea. Applied and Environmental Microbiology 73, 3348-3362.

Lucio, M., 2009. Datamining metabolomics: the convergence point of non-target approach and statistical investigation. http://nbn-resolving.de/urn:nbn:de:bvb:91-diss-20080916-673608-1-4.

Maatallah, M.' Vading, M., Kabir, M.H., Bakhrouf, A., Kalin, M., Nauclér, P., Brisse, S., Giske, C.G., 2009. *Klebsiella variicola* is a frequent cause of bloodstream infection in the Stockholm area, and associated with higher mortality compared to *K. pneumonia* . Mol Plant Pathol. 10, 325-335. doi: 10.1111/j.1364-3703.2009.00542.x.

Martinez, R.J., Mills, H.J., Story, S., Sobecky, P.A., 2006. Prokaryotic diversity and metabolically active microbial populations in sediments from an active mud volcano in the Gulf of Mexico. Environmental Microbiology 8, 1783-1796.

Mazzini, A., Etiope, G., 2017. Mud volcanism: An updated review. Earth-Science Reviews 168, 81-112. doi.org/10.1016/j.earscirev.2017.03.001

Meckenstock, R.U., von Netzer, F., Stumpp, C., Lueders, T., Himmelberg, A.M., Hertkorn, N., Schmitt-Kopplin, P., Harir, M., Hosein, R., Haque, S., Schulze-Makuch, D., 2014. Water droplets in oil are microhabitats for microbial life. Science 345, 673-676. doi:10.1126/science.1252215

Mieiro, C.L., Pato, P., Pereira, E., Mirante, F., Coutinho, J.A.P., Pinheiro, L.M., Magalhães, V.H., Duarte, A.C., Abuter, R., 2007. Total mercury in sediments from mud volcanoes in Gulf of Cadiz. Marine Pollution Bulletin 54, 1539-1544.

Milkov, A.V., Sassen, R., Apanasovich, T.V., Dadashev, F.G., 2003. Global gas flux from mud volcanoes: A significant source of fossil methane in the atmosphere and the ocean. Geophysical Research Letters 3, 1037-1040.

Miller, J.R., 2018. Morganella infections. https://emedicine.medscape.com/article/222443-overview#a0101, updated 29 Nov 2018.

Moradi, M., Song, Z., Tao, X. Introducing a novel bacterium, *Vibrio neocaledonicus* sp., with the highest corrosion inhibition efficiency. Electrochemistry Communications 51, 64-68.

Nadkarni M.A., Martin, F.E., Jacques, N.A., Hunter, N., 2002. Determination of bacterial load by real-time PCR using a broad-range (universal) probe and primers set. Microbiology 148, 257–266.

Niemann, H., Lösekann, T., de Beer, D., Elvert, M., Nadalig, T., Knittel, K., Amann, R., Sauter, E.J., Schlüter, M., Klages, M., Foucher, J.P., Boetius, A., 2006. Novel microbial communities of the Haakon Mosby mud volcano and their role as methane sink. Nature 443. doi:10.1038/nature05227.

Orlowski, N., Breuer, L., Angeli, N., Boeckx, P., Brumbt, C., Cook, C.S., Dubbert, M., Dyckmans, J., Gallagher,B., Gralher, B., Herbstritt, B., Hervé-Fernández,P., Hissler, C., Koeniger, P., Legout, A., Macdonald, C.J., Oyarzún, C., Redelstein, R., Seidler, C., Siegwolf, R., Stumpp, C., Thomsen, S., Weiler, M., Werner, C., McDonnell, J.J., 2018. Inter-laboratory comparison of cryogenic water extraction systems for stable isotope analysis of soil water. Hydrology and Earth System Sciences 22, 3619-3637. doi: 10.5194/hess-22-3619-2018

Parshina, S.N., Kleerebezem, R., Sanz, J.L., Lettinga, G., Nozhevnikova, A.N., Kostrikina, N.A., Lysenko, A.M., Stams, A.J., 2003. *Soehngenia saccharolytica gen. nov., sp. nov*. and *Clostridium amygdalinum sp. nov*., two novel anaerobic, benzaldehyde-converting bacteria. International Journal of Systematic and Evolutionary Microbiology 53, 1791–1799. doi:10.1099/ijs.0.02668-0.

Peters, E.J., 2011. Water quality of rainwater cisterns in the Grenadines. The West Indian Journal of Engineering 33, 56-64.

Plumlee, G.S., Casadevall, T.J., Wibowo, H.T., Rosenbauer, R.J., Johnson, C.A., Breit, G.N., Lowers, H.A., Wolf, R.E., Hageman, P.L., Goldstein, H., Anthony, M.W., Berry, C.J., Fey, D.L., Meeker, G.P., and Morman, S.A., 2008. Preliminary analytical results for a mud sample collected from the LUSI mud volcano, Sidoarjo, East Java, Indonesia: U.S. Geological Survey Open-File Report 2008-1019, Reston, VA, U.S.A. https://pubs.usgs.gov/of/2008/1019/pdf/OF08-1019_508.pdf.

Podder, M.P., Rogers, L., Daley, P.K., Keefe, G.P., Whitney, H.G., Tahlan, K., 2014. Klebsiella species associated with bovine mastitis in Newfoundland. PLoS ONE 9, *e106518*. Bibcode:2014PLoSO...9j6518P. doi:10.1371/journal.pone.0106518.

Poovorawan, K., Chatsuwan, T., Lakananurak, N., Chansaenroj, J., Komolmit, P., Poovorawan, Y., 2013. *Shewanella haliotis* associated with severe soft tissue infection, Thailand. Emerging Infectious Diseases 19, 1019–1021. doi:10.3201/eid1906.121607.

Ramamurthy, T., Chowdhury, G., Pazhani, G.P., Shinoda, S., 2014. *Vibrio fluvialis*: an emerging human pathogen. Front Microbiol. 5, 91. doi: 10.3389/fmicb.2014.00091

Reid, K.C., Cockerill, F.R., and Patel, R. (2001) Clinical and epidemiological features of *Enterococcus casseliflavus/flavescens* and *Enterococcus gallinarum* bacteremia: a report of 20 cases. *Clinical Infectious Diseases* 32: 1540–1546, doi.org/10.1086/320542

Reilly, G.D., Reilly, C.A., Smith, E.G., Baker-Austin, C., 2011. *Vibrio alginolyticus*-associated wound infection acquired in British waters, Guernsey. Euro Surveill. 16 (42).

Saunders, R., Mellowes, W., Clarke, R., Kimkeran, K., 2003. Application of SODIS technology to rain and tap water samples from Mayaro, Trinidad & Tobago, in Litter, M.I., Mansilla, H.D. (Eds.), Solar Disinfection of Water in Rural Communities of Latin America. Agencia Interamericana para la Coooperación y el Desarrollo, pp. 83-87. http://www.iiap.org.pe/upload/publicacion/PUBL438.pdf#page=84.

945 Sauter, E.J., Muyakshin, S.I., Charlou, L.C., Schlüter, M., Boetius, A., Jerosch, K., Damm, E.,
946 Foucher, J.-P., Klages, M., 2006. Methane discharge from a deep-sea submarine mud
947 volcano into the upper water column by gas hydrate-coated methane bubbles. Earth
948 Planet. Sci. Letters 243, 354-365.
949
950 Schmitt-Kopplin, P., Kiss, G., Dabek-Zlotorzynska, E., Gelencsér, A., Hertkorn, N., Harir,
951 M., Hong, Y., Gebefügi, I., 2010. Analysis of the unresolved organic fraction in
952 atmospheric aerosols with ultrahigh-resolution mass spectrometry and nuclear
953 magnetic resonance spectroscopy: organosulfates as photochemical smog constituents.
954 Anal Chem. 82, 8017–8026.
955
956 Schulze-Makuch, D., Goodell, P., Kretzschmar, T. Kennedy, J.F., 2003. Microbial and
957 chemical characterization of a groundwater flow system in an intermontane basin of
958 southern New Mexico. Hydrogeology Journal 11, 401-412.
959
960 Selesi, D., Schmid, M., Hartmann, A., 2005. Diversity of green-like and red-like ribulose-1,5-
961 bisphosphate carboxylase/oxygenase large-subunit genes (cbbL) in differently
962 managed agricultural soils. Appl. Environ. Microbiol. 71, 175–184
963
964 Selesi, D., Pattis, I., Schmid, M., Kandeler, E., Hartmann, A., 2007. Quantification of
965 bacterial Rubisco genes in soil by cbbL targeted real-time PCR. J. Microbiol. Methods
966 69, 497–503. doi: 10.1016/j.mimet.2007.03.002.
967
968 Smith, G.A., Nickels, J.S., Kerger, R., 1986. Quantitative characterization of microbial
969 biomass and community structure in subsurface material: a prokaryotic consortium
970 responsive to organic contamination. Can J Microbiol 32, 104-111.
971
972 Smith, C.J., Nedwell, D.B., Dong, L.F., Osborn, A.M., 2007. Diversity and abundance of
973 nitrate reductase genes (narG and napA), nitrite reductase genes (nirS and nrfA), and
974 their transcripts in estuarine sediments. Appl Environ Microbiol. 73, 3612–3622.
975
976 Steinberg, L.M., Regan, J.M., 2008. Phylogenetic comparison of the methanogenic
977 communities from an acidic, oligotrophic fen and an anaerobic digester treating
978 municipal wastewater sludge. Appl Environ Microbiol 74, 6663–6671.
979
980 Sundar, R., Darsan, J., 2019, A geomorphological analysis of the Piparo and Digity mud
981 volcanoes in south Trinidad. Caribbean Journal of Earth Science 49, 23-34.
982
983 Tziotis, D., Hertkorn, N., Schmitt-Kopplin, P., 2011. Kendrick-analogous network
984 visualization of ion cyclotron resonance Fourier transform mass spectra: improved
985 options for the assignment of elemental compositions and the classification of organic
986 molecular complexity. EJMS 17, 415-421
987
988 Welch, P., David, J., Clarke, W., Trinidade, A., Penner, D., Bernstein, S., Mcdougall, L., and
989 Adesiyun, A.A., 2000. Microbial quality of water in rural communities of Trinidad.
990 Pan American Journal of Public Health 8, 172-180.
991
992 White, D.C., Flemming, C.A., Leung, K.T., Macnaughton, S.J., 1998. In situ microbial
993 ecology for quantitative appraisal, monitoring, and risk assessment of pollution
994 remediation in soils, the subsurface, the rhizosphere and in biofilms. J. Microbiol.
995 Method 32, 93-105.

Yakimov, M.M., Giuliano, L., Crisafi, E., Chernikova, T.N., Timmis, K.N., Golyshin, P.N., 2002. Microbial community of a saline mud volcano at San Biagio-Belpasso, Mt. Etna